

**inter.noise 2000**

*The 29th International Congress and Exhibition on Noise Control Engineering  
27-30 August 2000, Nice, FRANCE*

---

I-INCE Classification: 1.0

## **NOZZLE DESIGN EFFECT ON VORTEX INDUCED INSTABILITIES IN AN AXIAL INJECTED COLD FLOW MODEL OF THE ARIANE-5 EAP**

**J. Anthoine, D. Yildiz, J.-M. Buchlin**

von Karman Institute, Chaussee de Waterloo, 72, 1640, Rhode-Saint-Genese, Belgium

Tel.: +32 2 359 96 11 / Fax: +32 2 359 96 00 / Email: anthoine@vki.ac.be

**Keywords:**

FLOW-ACOUSTIC COUPLING, ARIANE 5 BOOSTER, EXPERIMENTAL APPROACH, CAVITY NOISE

**ABSTRACT**

The nozzle design effect on sound production is investigated at the VKI to improve the understanding of the aeroacoustic coupling that occurs in the Ariane-5 booster. Acoustic pressure measurements are carried out in a purely axial cold flow model. Flow-acoustic coupling on the second longitudinal acoustic mode is observed for all the nozzles including cavity. Furthermore, the maximum resonance amplitude is highly dependent on the nozzle design. The evolution of the sound pressure levels is approximately linear with the cavity volume. Without cavity, the fluctuations are damped by at least one order of magnitude.

**1 - INTRODUCTION**

The aeroacoustics of solid propellant boosters is investigated at the von Karman Institute as a part of a CNES program related to the Ariane-5 EAP [1,2,3]. This accelerator has a segmented combustion chamber consisting of three cylindrical segments and a submerged nozzle. Two inhibitor rings ensuring thermal protection separate the three segments. The hot burnt gas flow originates radially from the burning surface of the combustion chamber and develops longitudinally before reaching the exhaust nozzle. During the combustion, the regression of the burning surface is faster than the inhibitor rings that become obstacles into the flow-field producing high shear regions where vortex shedding may be generated. This mechanism drives oscillation if the shedding is coupled to one of the acoustic resonant modes of the motor chamber. Pressure oscillations have been already observed for solid rocket motors, such as the Titan IV and the Ariane-5 EAP [4,5,6]. They reach a maximum when the vortex shedding frequency is close to a longitudinal acoustic mode frequency of the chamber.

**2 - THE FLOW-ACOUSTIC COUPLING**

The oscillations are linked to the hydrodynamic instability of the sheared regions of the flow and to the coupled response of the motor [7]. It is now well established that unstable oscillations are produced by the combination of the following mechanisms:

- Hydrodynamic instability of shear regions of the flow.
- Roll-up, growth and advection of vortices.
- Impingement of the vortices on a surface located downstream such as the nozzle head and generation of an acoustic perturbation.
- Acoustic propagation from the downstream source.
- Transfer of energy from the acoustic mode to the shear flow instability.

The generation of self-sustained sound resonance in a tube depends on the phase of the acoustic oscillation at which a vortex shed by the upstream obstacle reaches the downstream one [8]. In the present model, the upstream obstacle is the inhibitor while the downstream one is the nozzle. This phase is determined by the time needed by a vortex to cover the distance between the obstacles, and is therefore a function of this distance and of the speed at which flow disturbances travel. When resonance occurs, the selection of the acoustic mode depends on the relative position  $l/L$  of the inhibitor compared to the acoustic mode shape. Indeed, to guarantee the highest sound pressure levels, the inhibitor must be as close as possible to an acoustic pressure node (highest acoustic velocity fluctuations) to obtain a maximum of acoustic receptivity at the inhibitor. Therefore, the coupling will occur for that acoustic mode only when an integer number of vortices are present between the inhibitor and the nozzle.

### 3 - THE EXPERIMENTAL SET-UP

The experimental facility is a 1/30-scale modular axisymmetric cold flow model of the Ariane-5 solid rocket motor, with a fully axial flow. The model, sketched in figure 1, consists of a cylindrical test section, with an inhibitor, and a submerged nozzle with sonic condition at the throat [1], [9]. The internal diameter  $D$  of the test section, equal to 76 mm, is based on the 1/30-scale similarity with the full-scale motor obtained by conserving the Mach number when 50% of the propellant is burnt. The total length  $L$  and the inhibitor parameters ( $d$  &  $l$ ) can be modified. The test section is supplied with compressed air. The temperature of the fluid in the test section is around 285K, while the static pressure is varying between  $1.7 \times 10^5$  Pa and  $4.2 \times 10^5$  Pa depending on the Mach number  $M_0$ . The minimum static pressure value guarantees sonic conditions at the nozzle throat. The circulation of the air along all the connected pipes produces acoustic noise that could interact with the acoustic measurements carried out in the test section. The insertion of a porous plate at the inlet of the test section aims to ensure an acoustic insulation of the test section from the air supply, by providing a high pressure drop [9]. This pressure drop is of the order of magnitude of the static pressure in the test section.

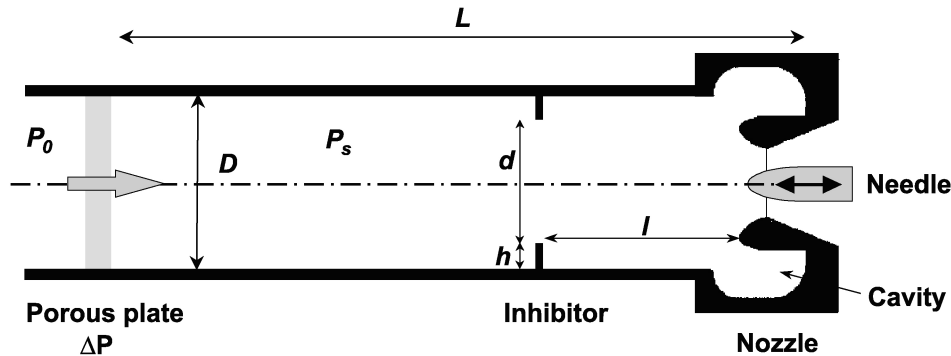


Figure 1: The 1/30-scale modular axisymmetric setup for purely axial injected flow.

In the Ariane-5 booster, the flow-acoustic coupling is characterized by a shift of the instability mode frequency with respect to time and a frequency jump between the instability modes. Time evolution should then be considered in the experiments. As the combustion is radial, time varies as the inverse of the Mach number in the segments. Therefore, flow acoustic coupling is identified by plotting the evolution of the Strouhal number in function of the Mach number [4]. The only way to vary the Mach number is to change in a continuous manner the nozzle throat area, by means of a movable needle (figure 1), [9].

The objective of the research is to investigate the influence of the nozzle geometry on the sound production. Different nozzle geometries are designed. They are sketched in figure 2. Nozzle 1 is the submerged nozzle representing the real geometry at 1/30 scale. For the second nozzle, a part of the cavity is filled. The cavity volume is reduced by 49% and the cavity depth by 60%, changing slightly the total length of the test section. In the third one, the cavity is filled up to the nozzle head. The nozzle lip has disappeared but the backward facing step at the end of the segment is still present. The fourth nozzle has to be compared to the second one: the backward facing step disappeared by keeping a segment of 76 mm diameter till the far end of the cavity. Comparing nozzles 3 and 4 to nozzle 2 will show if the pressure fluctuations are more amplified by the presence of a nozzle lip or by the backward facing step. For nozzle 5, the lip geometry is changed compared to nozzle 2, while nozzle 6 is only the convergent-divergent section, without cavity. For all these nozzles, the throat diameter is equal to 30 mm and the convergent

and divergent part keeps the same geometries. The only differences are coming from the cavity. Nozzles 7 and 8 are identical to nozzles 1 and 6 respectively, with a throat diameter of 37 mm. Finally, nozzle 9 is designed to provide a cavity volume of 20% higher than nozzle 7. The cavity, which starts at the nozzle head, is not deeper but larger than the one of nozzle 7. So, the vortices will interact with the nozzle head before feeling the widening of the segment into a cavity.

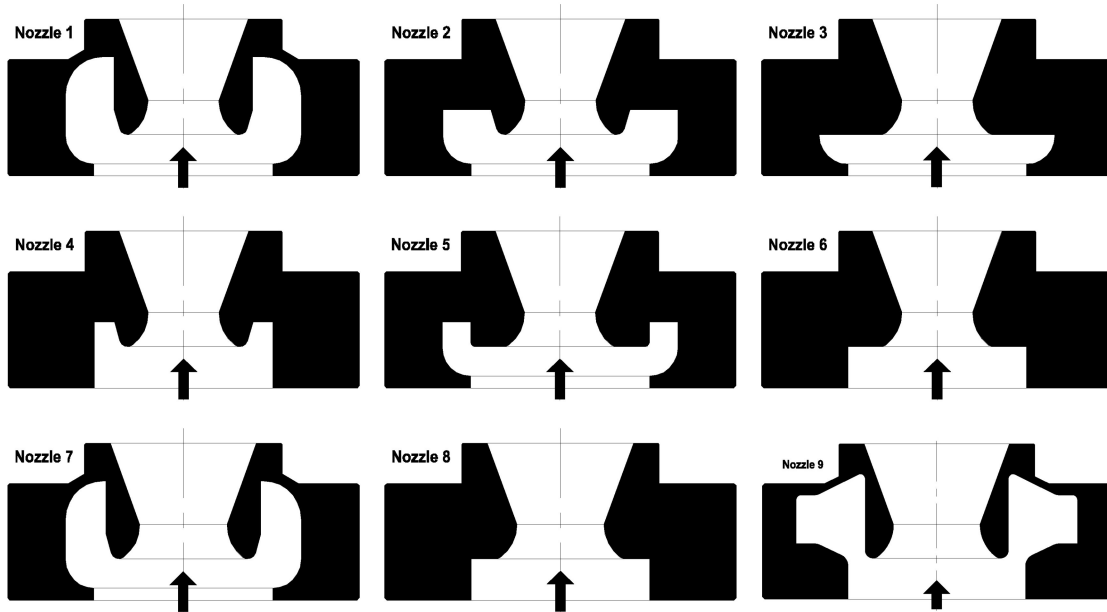


Figure 2: Drawings of the different exhaust nozzle geometries.

Piezoelectric pressure probes (PCB) from Piezotronics Inc. allow the measurement of the acoustic pressure fluctuations. A first probe is placed just downstream of the porous plate. A second probe is mounted between the inhibitor and the nozzle. Finally, for the submerged nozzle (nozzle 1), a third probe is placed on the wall of the nozzle cavity. The acoustic pressure fluctuation data are acquired by means of a DAS1601 acquisition card controlled by TESTPOINT<sup>®</sup>. The signals are filtered at 3 kHz and acquired at 7.5 kHz. 16384 samples are saved on the disk and analyzed to determine the power spectrum of the pressure fluctuations. The spectrum is averaged on 7 blocks of 4096 data with an overlapping of 0.5. It gives a frequency resolution of 1.8 Hz.

#### 4 - THE NOZZLE DESIGN EFFECT ON SOUND PRESSURE LEVEL

The flow-acoustic feedback loop relies upon the interaction between the vortices and the nozzle. The nozzle geometry is then expected to play an important role in the amplification of the sound pressure fluctuations.

##### 4.1 - Pressure fluctuations at the forward end of the test section

Pressure fluctuations are measured for an inhibitor of  $d=58$  mm placed at  $l=71$  mm from the head of the nozzle and for a test section length  $L$  around 393 mm. The maximum pressure fluctuation values are plotted versus Mach number  $M_0$  in figure 3a for all the nozzles with a throat diameter of 30 mm. The evolution of the Strouhal number ( $St_a = fl/a$ ) corresponding to the maximum of the pressure fluctuations is given in figure 3b where the horizontal lines correspond to the theoretical acoustic modes of the test section.

A flow-acoustic coupling is identified when the excited frequency crosses an acoustic mode of the chamber and jumps to another acoustic mode. The variation of the Strouhal number is similar for all the nozzles except for number 6, without cavity. That means that the vortex shedding does excite the second longitudinal acoustic mode within the same Mach number range for all the nozzles. The maximum of sound pressure levels that corresponds to the maximum of coupling appears at  $M_0=0.08$  whatever the nozzle geometry. Moreover, the amplitude of the maximum resonance is highly dependent on the nozzle design. For nozzle 1 (with cavity), each time the excited frequency is close to an acoustic mode frequency, the pressure fluctuation level is amplified. The maximum is reached when crossing the acoustic mode. When the nozzle cavity volume decreases (nozzle 2), the pressure fluctuation lessens. The influence of

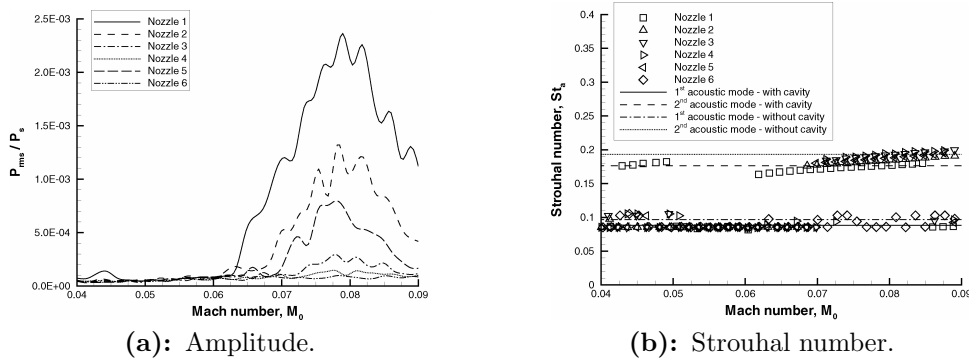


**Figure 3:** Evolutions of the maximum pressure fluctuation for nozzles with 30 mm throat diameter (nozzles 1 to 6).

the backward facing step at the end of the segment and of the nozzle head is depicted in comparing nozzle 2 to nozzles 3 and 4, respectively. For nozzles 3 and 4, the pressure level is reduced but the decrease is more important for nozzle 4. The amplitude measured for nozzle 4 is similar to that obtained for the nozzle without cavity (nozzle 6). Finally, the effect of nozzle head geometry is shown by nozzle 5. This nozzle presents a smaller cavity volume than nozzle 2 that results in fainter pressure fluctuations compared to nozzle 2. So, the cavity volume plays an important role in the amplification of the pressure fluctuation. To quantify this influence, table 1 yields a comparison between the nozzle cavity volume and the maximum pressure level. Only the nozzles presenting a cavity are considered. The volume and pressure amplitude are given in absolute value and relative to nozzle 1. The sound pressure level increases quite linearly with the nozzle cavity volume.

Nozzle	Cavity volume		Maximum sound pressure level	
	[x 10 <sup>-6</sup> m <sup>3</sup> ]	ratio	[x 10 <sup>-3</sup> ]	ratio
1	203.5	1	2.3	1
2	104.3	0.51	1.25	0.54
5	67.1	0.33	0.8	0.35

**Table 1:** Comparison between the nozzle cavity volumes and the maximum pressure levels.

#### 4.2 - Pressure fluctuations at the backward end of the test section

The pressure fluctuations along the test section have also been measured by using probes flush mounted at different locations: just downstream the porous plate, between the inhibitor and the nozzle and in the nozzle cavity. They are compared in figure 4. These results are obtained for the nozzle 7 with a throat diameter of 37 mm. The signal acquired just downstream the porous plate (forward end) corresponds to the result presented before. The only modes excited at the forward end of the test section are the longitudinal acoustic modes (based on L). Another frequency, equal to 1875 Hz and corresponding to a Strouhal number of 0.4, is also detected using a probe located in the nozzle cavity. That frequency does not correspond to any longitudinal acoustic mode frequency. The signal of the probe placed between the inhibitor and the cavity shows that frequency is also excited, but with a smaller amplitude. Therefore, this resonance should come from the excitation of an acoustic mode of the nozzle cavity as it can only be measured in the cavity or close to it. When occurring, this resonance produces sound pressure levels about 10 times larger than those measured at the longitudinal acoustic modes of the test section. Notice also that the corresponding range of Mach number is narrower.

To explain such a high frequency, the nozzle cavity can be modeled as an opened-closed tube (figure 2, nozzle 1). This should provide a rough estimate of the excited frequency. Then, the theoretical value of the acoustic mode frequency is given by  $f_{ac,c} = a / (4L_c)$  where  $a$  is the speed of sound and  $L_c$  is the length of the "ideal" tube.  $f_{ac,c}$  is equal to 1878 Hz for an experimental cavity of 45 mm length, which is very close to the experimental value of 1875 Hz. So, the peak appearing at Mach number of 0.11 corresponds to the excitation of the cavity itself.

## 5 - CONCLUSIONS

The effect of the nozzle design of the Ariane-5 MPS on sound production is investigated at the VKI to improve the understanding of the aeroacoustic coupling. Acoustic pressure measurements are carried out

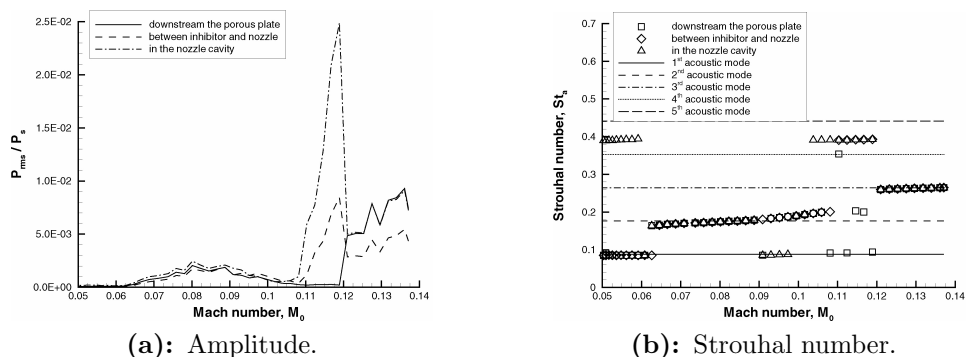


**Figure 4:** Evolutions of the maximum pressure fluctuation at different locations along the test section wall for nozzle 7.

in a purely axial cold flow model, for different nozzle geometries. Flow-acoustic coupling is observed only for nozzles including cavity. The vortex shedding excites the second longitudinal acoustic mode within the same Mach number range for all the nozzles with cavity. The maximum of sound pressure that appears at  $M_0=0.08$  is highly dependent on the nozzle design. The sound pressure level is approximately a linear function of the cavity volume. Without cavity, the fluctuations are damped by at least one order of magnitude.

#### Future work

The investigation continues to analyze if the nozzle design has still an effect on the amplification of pressure fluctuations in presence of radial injected flow. A new experimental facility with a radial injection through porous cylinders, which simulates the hot bunt gas from the propellant combustion, is tested.

#### ACKNOWLEDGEMENTS

This work was supported by the European Space Agency (ESA) and by the Centre National d'Etudes Spatiales (CNES). It is a part of a research program coordinated by the CNES and ONERA (Office National d'Etudes et de Recherches Aérospatiales). The authors are grateful to M. J. Gigou from ESA and to MM. R. Bec and S. Radulovic from the CNES.

#### REFERENCES

1. **J. Anthoine, O. Repellin, J-M. Buchlin and D. Olivari**, The Ariane 5 MPS Aeroacoustics Research at VKI: an Overview, In *1st European Conference on Launcher Technology "Launch Vehicle Vibrations"*, Toulouse, France, pp. 569-578, 1999
2. **J. Anthoine, J-M. Buchlin and J-F. Guery**, Experimental and Numerical Investigations of Nozzle Geometry Effect on the Instabilities in Solid Propellant Boosters, In *36th AIAA/ASME/SAE/ASEE Joint Propulsion Conference and Exhibit, Huntsville, Alabama, AIAA Paper 2000-3560*, 2000
3. **J. Anthoine, M. Mettenleiter, O. Repellin, J-M. Buchlin and S. Candel**, Influence of Adaptive Control on Vortex Driven Instabilities in a Scaled Model of Solid Propellant Motors, *under consideration for publication in the Journal of Fluid Mechanics*
4. **K.W. Dotson, S. Koshigoe and K.K. Pace**, Vortex Shedding in a Large Solid Rocket Motor Without Inhibitors at the Segment Interfaces, *Journal of Propulsion and Power*, Vol. 13 (2), pp. 197-206, 1997
5. **S. Scippa, P. Pascal and F. Zanier**, Ariane-5-MPS: Chamber Pressure Oscillations Full Scale Firings Results Analysis and Further Studies, In *AIAA Paper 94-3068*, 1994
6. **J-C. Traineau, M. Prévost, F. Vuillot, P. Le Breton, J. Cuny, N. Preioni and R. Bec**, A Subscale Test Program to Assess the Vortex Shedding Driven Instabilities in Segmented Solid Rocket Motors, In *AIAA Paper 97-3247*, 1997
7. **G.A. Flandro and H.R. Jacobs**, Vortex Generated Sound in Cavities, In *AIAA Paper 73-1014*, 1973

8. **K. Hourigan, M.C. Welsh, M.C. Thompson and A.N. Stokes**, Aerodynamic sources of acoustic resonance in a duct with baffles, *Journal of Fluids and Structures*, Vol. 4 (4), pp. 345-370, 1990
9. **J. Anthoine and D. Olivari**, Cold Flow Simulation of Vortex Induced Oscillations in a Model of Solid Propellant Boosters, In *5th AIAA/CEAS Aeroacoustics Conference, Greater Seattle, Washington, AIAA Paper 99-1826*, 1999